

A new species of forest hedgehog (*Mesechinus*, Erinaceidae, Eulipotyphla, Mammalia) from eastern China

Zifan Shi¹, Hongfeng Yao¹, Kai He², Weipeng Bai³, Jiajun Zhou⁴, Jingyi Fan¹, Weiting Su⁵, Wenhui Nie⁵, Shuzhen Yang⁶, Kenneth O. Onditi⁵, Xuelong Jiang⁵, Zhongzheng Chen^{1,5}

1 Collaborative Innovation Center of Recovery and Reconstruction of Degraded Ecosystem in Wanjiang Basin Co-founded by Anhui Province and Ministry of Education, School of Ecology and Environment, Anhui Normal University, Wuhu, China

2 Key Laboratory of Conservation and Application in Biodiversity of South China, School of Life Sciences, Guangzhou University, Guangzhou, China

3 Institute of Nihewan Archaeology, College of History and Culture, Hebei Normal University, Shijiazhuang, China

4 Zhejiang Forest Resources Monitoring Center, Hangzhou, China

5 State Key Laboratory of Genetic Resources and Evolution & Yunnan Key Laboratory of Biodiversity and Ecological Security of Gaoligong Mountain, Kunming Institute of Zoology, Chinese Academy of Sciences, Kunming, China

6 Management Office, National Nature Reserve of Mount Tianmu, Hangzhou, China

Corresponding author: Zhongzheng Chen (zhongzheng112@126.com)

Academic editor: Alessio Iannucci

Abstract

The hedgehog genus *Mesechinus* (Erinaceidae, Eulipotyphla) is currently comprised of four species, *M. dauuricus*, *M. hughi*, *M. miodon*, and *M. wangi*. Except for *M. wangi*, which is found in southwestern China, the other three species are mainly distributed in northern China and adjacent Mongolia and Russia. From 2018 to 2023, we collected seven *Mesechinus* specimens from Anhui and Zhejiang provinces, eastern China. Here, we evaluate the taxonomic and phylogenetic status of these specimens by integrating molecular, morphometric, and karyotypic approaches. Our results indicate that the Anhui and Zhejiang specimens are distinct from the four previously recognized species and are a new species. We formally described it here as *Mesechinus orientalis* sp. nov. It is the only *Mesechinus* species occurring in eastern China and is geographically distant from all known congeners. Morphologically, the new species is most similar to *M. hughi*, but it is distinguishable from that species by the combination of its smaller size, shorter spines, and several cranial characteristics. *Mesechinus orientalis* sp. nov. is a sister to the lineage composed of *M. hughi* and *M. wangi* from which it diverged approximately 1.10 Ma.

Key words: Anhui, mammals, phylogeny, taxonomy

Introduction

In recent years, interest in the faunal inventory of insectivorous mammals in different countries has increased (Kryštufek and Motokawa 2018; Andreychev and Kuznetsov 2020). The forest hedgehog genus *Mesechinus* Ognev, 1951 is one of five extant genera in the subfamily Erinaceinae. *Mesechinus* was previously regarded as a subgenus of *Erinaceus* Linnaeus, 1758 or *Hemiechinus* Fitzinger, 1866 (Pavlinov and Rossolimo 1987; Corbet 1988; Bannikova et al. 2002). Frost et al. (1991) promoted it to full-genus status, a conclusion supported



Received: 24 August 2023
Accepted: 6 November 2023
Published: 28 November 2023

ZooBank: <https://zoobank.org/6D64FC0C-9992-42FB-A146-F6192FE7A104>

Citation: Shi Z, Yao H, He K, Bai W, Zhou J, Fan J, Su W, Nie W, Yang S, Onditi KO, Jiang X, Chen Z (2023) A new species of forest hedgehog (*Mesechinus*, Erinaceidae, Eulipotyphla, Mammalia) from eastern China. ZooKeys 1185: 143–161. <https://doi.org/10.3897/zookeys.1185.111615>

Copyright: © Zifan Shi et al.
This is an open access article distributed under terms of the Creative Commons Attribution License ([Attribution 4.0 International – CC BY 4.0](https://creativecommons.org/licenses/by/4.0/)).

by analysis of morphological characters (Gould 1995) and chromosomal data (Korablev et al. 1996). The most distinctive morphological character distinguishing *Mesechinus* from *Erinaceus* and *Hemiechinus* is the unique shape of the suprameatal fossa; the lateral border of this fossa is somewhat U-shaped in *Mesechinus* but C-shaped in the other erinaceine genera (Frost et al. 1991).

Currently, four species are recognized in the genus, including *M. dauuricus* (Sundevall, 1842), *M. hughii* (Thomas, 1908), *M. miodon* (Thomas, 1908), and *M. wangi* He, Jiang & Ai, 2018 (Wilson and Mittermeier 2018). *Mesechinus* species mainly occur in northern China and adjacent Mongolia and Russia, with an isolated species (*M. wangi*) on Mount Gaoligong, Yunnan, southwestern China (Frost et al. 1991; Ai et al. 2018). *Mesechinus dauuricus* and *M. hughii* mainly inhabit semidesert habitats, including cold-temperate deciduous and temperate deserts, warm-temperate deserts, grasslands and deciduous broad-leaf forests, *M. miodon* mainly inhabits semiarid and dry steppe habitats and subalpine and low-elevation coniferous forests, and only *M. wangi* inhabits tropical or subtropical rainforest (Ai et al. 2018; Wilson and Mittermeier 2018).

Hugh's Hedgehog (*M. hughii*) is the smallest species of *Mesechinus* and is mainly distributed in southern Shaanxi, southern Shanxi, and northern Sichuan in China (Ai et al. 2018) (Fig. 1). This dark-coloured hedgehog with no all-white spines was first described by Thomas (1908) based on specimens from Paochi (= Baoji), Shaanxi, China. Chen et al. (2020) reported the first record of *M. hughii* in eastern China based on a specimen collected from Xuancheng, Anhui Province. They pointed out that Anhui *Mesechinus* specimen

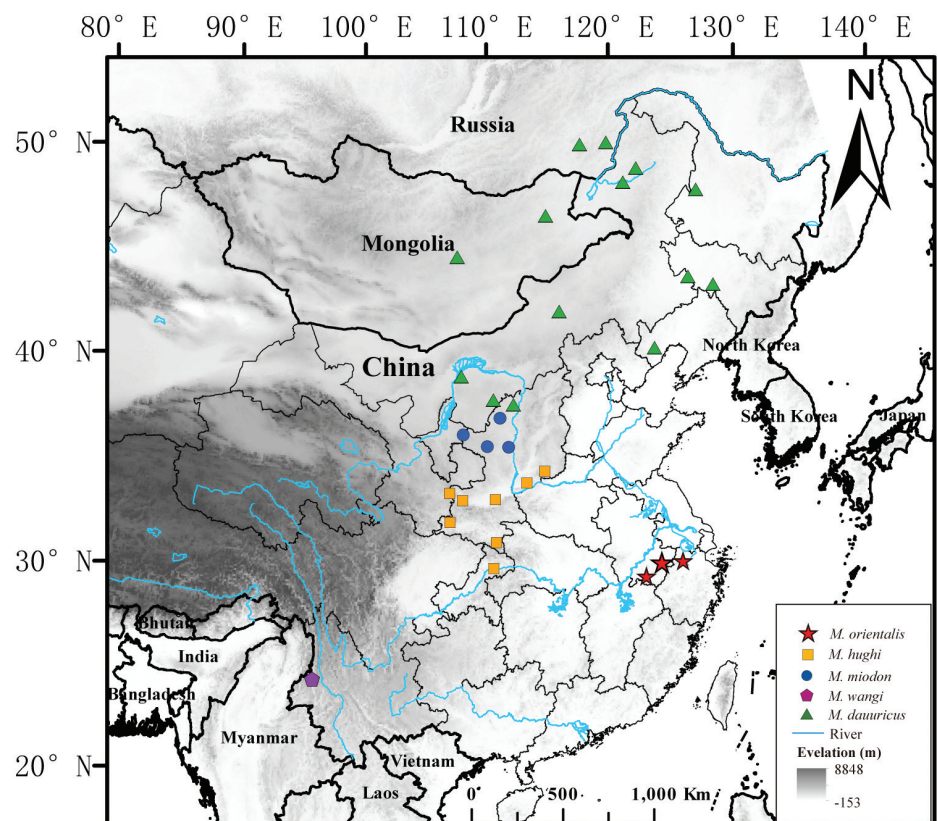


Figure 1. Distribution of the genus *Mesechinus*.



Figure 2. A living *Mesechinus orientalis* sp. nov. (XC 2205003) from Xuancheng, Anhui.

was genetically distant from Shaanxi specimens (4.9–5.3% of CYT B gene) and may have undergone isolated differentiation (Chen et al. 2020). Recently, we obtained a CYT B sequence of *M. wangi*. Our preliminary phylogenetic analysis revealed that the Anhui specimens form a lineage sister to the lineage composed of *M. hughi* from Shaanxi and *M. wangi*, which suggests that additional studies with more specimens were necessary to confirm the taxonomic status of the Anhui *Mesechinus*.

From 2022 to 2023, we collected six specimens of *Mesechinus* from Anhui and Zhejiang provinces, eastern China (Fig. 2). Our morphological and molecular results reveal the eastern China samples differ from *M. hughi* and other known *Mesechinus* species. We recognize it as a new species, *Mesechinus orientalis* sp. nov., which we describe here.

Materials and methods

Sampling

Seven *Mesechinus orientalis* sp. nov. specimens, including a specimen collected by Chen et al. (2020), were obtained from Anhui and Zhejiang provinces in eastern China (Suppl. material 1). Our specimens were euthanized, and liver or muscle tissues were extracted and preserved in pure ethanol. Skulls were extracted and cleaned. All the specimens and tissues were deposited at Anhui Normal University (AHNU). Animals were handled consistent with the Guidelines of the American Society of Mammalogists (Sikes 2016).

Morphological measurement and analysis

Five external measurements, including weight (W), head–body length (HB), tail length (TL), hind-foot length (HF), and ear length (EL) of *M. orientalis* sp. nov. were measured in the field to the nearest 1 g or 1 mm. Twelve craniodental variables were measured using digital calipers graduated to 0.01 mm following Pan et al. (2007) and Ai et al. (2018): greatest length of the skull (GLS), condylobasal length (CBL), basal length (BL), cranial height (CH), palatal length (PL), zygomatic breadth (ZMB), interorbital breadth (IOB), mastoid width (MTW), greatest width of nasal (GWN), breadth of first upper molar (BM1), length of upper tooth row (LUTR), and length of below tooth row (LBTR). Comparative morphological data of other *Mesechinus* species were obtained from Ai et al. (2018), which included 4 *M. wangji*, 18 *M. miodon*, 31 *M. hughi*, and 13 *M. dauuricus*.

Thirty-seven complete skulls were used for PCA, including specimens of 3 *M. wangji*, 20 *M. hughi*, 6 *M. miodon*, 1 *M. dauuricus*, and 7 *M. orientalis* sp. nov. Morphometric variation was analyzed using a principal component analysis (PCA) in SPSS 19.0 based on 12 \log_{10} -transformed cranial measurements. To further confirm the validity of the potential new species, we coded the characters of *Mesechinus* species according to Gould (1995). In this procedure, we systematically compared the morphological characteristics of the new species with other *Mesechinus* species, especially the most morphologically similar species, *M. hughi*.

Mitogenome sequencing, assembly, and annotation

We used next-generation sequencing (NGS) to obtain the complete mitochondrial genome of *M. orientalis* sp. nov. Illumina high-throughput sequencing platform was employed for sequencing with a strategy of 150 paired-ends, and the quality was checked using FastQC (de Sena Brandine and Smith 2021). The mitochondrial genome assembly was performed using NOVOPlasty (Dierckxsens et al. 2017).

The mitochondrial genome was annotated using MitoZ in the MITOS Web-Server with analytical parameters set using the vertebrate genetic code (Bernt et al. 2013; Meng et al. 2019). Geneious v. 9.0.2 (Kearse et al. 2012) was used to examine all mitochondrial genes. The obtained sequences were edited and aligned with MEGA v. 11 (Tamura et al. 2021). The newly obtained mitogenome has been deposited in GenBank (accession number [OR774964](https://www.ncbi.nlm.nih.gov/nuccore/OR774964)).

Phylogenetic analysis

The mitochondrial genomes of four other *Mesechinus* species, and six erinaceid species, including representatives of *Paraechinus* Trouessart, 1879, *Hemiechinus*, and *Atelerix* Pomel, 1848, were downloaded from GenBank and included in our analyses. Mitochondrial genomes of *Neotetracus sinensis* Trouessart, 1909 and *Hylomys suillus* Müller, 1840, also obtained from GenBank, were used as the outgroup (Table 1). The phylogenetic analyses were conducted using the two rRNA and 12 coding genes on the heavy chain and excluded ND6 on the light chain. Each gene was aligned using MUSCLE and then checked manually.

To reconstruct the phylogenetic relationships, maximum-likelihood (ML) and Bayesian-inference (BI) analyses were performed in IQ-TREE and MrBayes,

Table 1. Samples used for molecular phylogenetic analysis in this study.

Subfamily	Species	Museum code	Collection localities	GenBank no.
Galericinae	<i>Hylomys suillus</i>		Java, Indonesia	AM905041
	<i>Neotetracus sinensis</i>		Pingshan, Yibin, Sichuan, China	NC_019626
Erinaceinae	<i>Paraechinus micropus</i>	USNM369316		OP654708
	<i>Hemiechinus auritus</i>			AB099481
	<i>Atelerix albiventris</i>	USNM325883		OP654703
	<i>Erinaceus amurensis</i>		Gongwon, Korea	KX964606
	<i>Mesechinus miodon</i>		Yulin, Shaanxi, China	KT824773
	<i>M. dauuricus</i>	KIZ200908002		OP654710
	<i>M. wangi</i>	GLGS0907001		OP654712
	<i>M. hughi</i>	KIZ200908004		OP654727
	<i>M. orientalis</i> sp. nov.	XC 2205003	Xuancheng, Anhui, China	OR774964

respectively, in PhyloSuite (Zhang et al. 2020). The phylogenetic tree was visualized and annotated in tvBOT (Xie et al. 2023). The best-fit partitioning schemes were estimated based on the Bayesian Information Criterion (BIC) using PartitionFinder 2 (Lanfear et al. 2017).

Divergence time estimation

BEAST v. 2.6 (Bouckaert et al. 2014) was used to estimate divergence times in the CIPRES Science Gateway (Miller et al. 2015). The data were partitioned according to the results of PartitionFinder 2 (Suppl. material 2). We used the unlinked site model and linked clock model and time tree across partitions, and the relaxed lognormal clock model and a birth-death model for the tree prior. Two secondary calibrations were used: (1) the most recent common ancestor of the subfamilies Galericinae and Erinaceinae, which was estimated at ca 28.3–48.8 Ma (Meredith et al. 2011) using a lognormal distribution prior (mean = 3.61, SD = 0.142, offset = 0); and (2) The most recent common ancestor of Erinaceinae, which was estimated at ca 6.97 Ma (He et al. 2021), with a normal distribution prior (mean = 6.97, sigma = 2.05, offset = 0). The analyses were conducted twice, each for 100 million generations, sampling every 10000 generations. The posterior distribution of each parameter in the log file was estimated using Tracer v. 1.7 (Rambaut et al. 2018) to ensure that the effective sampling size of all parameters was greater than 200. For all BEAST analyses, we compiled time trees with TreeAnnotator v. 2.6 (Bouckaert et al. 2014) and excluded 10% of each chain as burn-in. The generated tree was viewed in FigTree v. 1.4 (Rambaut 2017) and beautified in tvBOT (Xie et al. 2023).

Cell culture and karyotype analysis

A female individual of *M. orientalis* sp. nov. (XC 2205003) collected in May 2022 was used for cell cultures. Standard procedures were applied for fibroblast culture, chromosome preparation, and G-banding. Two fibroblast cell lines derived from *M. orientalis* sp. nov. (XC 2205003) were established and deposited in the Kunming Cell Bank, Yunnan, China. A CytoVision system (Applied Imaging Co.,

USA) with a CCD camera mounted on a Zeiss microscope (Germany) was used to karyotype analysis. Chromosomes of *M. orientalis* sp. nov. (XC 2205003) were numbered according to *M. wangi* (Ai et al. 2018).

Results

Morphological analyses

Summaries of external morphology and craniodental measurements are given in Table 2. According to the measurements, *Mesechinus orientalis* sp. nov. (HB = 188.83 mm \pm 8.13; GLS = 49.95 mm \pm 1.69) is similar in size to *M. hughi* (HB = 189.71 mm \pm 23.80; GLS = 49.39 mm \pm 1.54) but much smaller than *M. wangi*, *M. dauricus*, and *M. miodon* (Table 2).

The first two PCA axes had eigenvalues exceeding 1.0 (Table 3). The first principal component (PC1) accounted for 69.32% of the total variance and was positively correlated with all variables (loading > 0.69), reflecting a size effect. The second principal component (PC2) accounted for 10.01% of the variance and was strongly positively correlated with GWN, MTW, and BM1 (loading > 0.53). The PC1 vs PC2 scatter plot (Fig. 3) showed *M. orientalis* sp. nov. slightly overlapping with *M. hughi* but well separated from *M. wangi*, *M. dauricus*, and *M. miodon*. Specimens of *M. orientalis* sp. nov. and *M. hughi* mainly occupy the negative regions of PC1, reflecting their smaller size compared to *M. wangi* and *M. miodon*. *Mesechinus orientalis* sp. nov. plotted on the positive regions of PC2, whereas most *M. hughi* specimens plotted on the negative regions, suggesting the new species has wider nasal, mastoid, and M¹ than *M. hughi*.

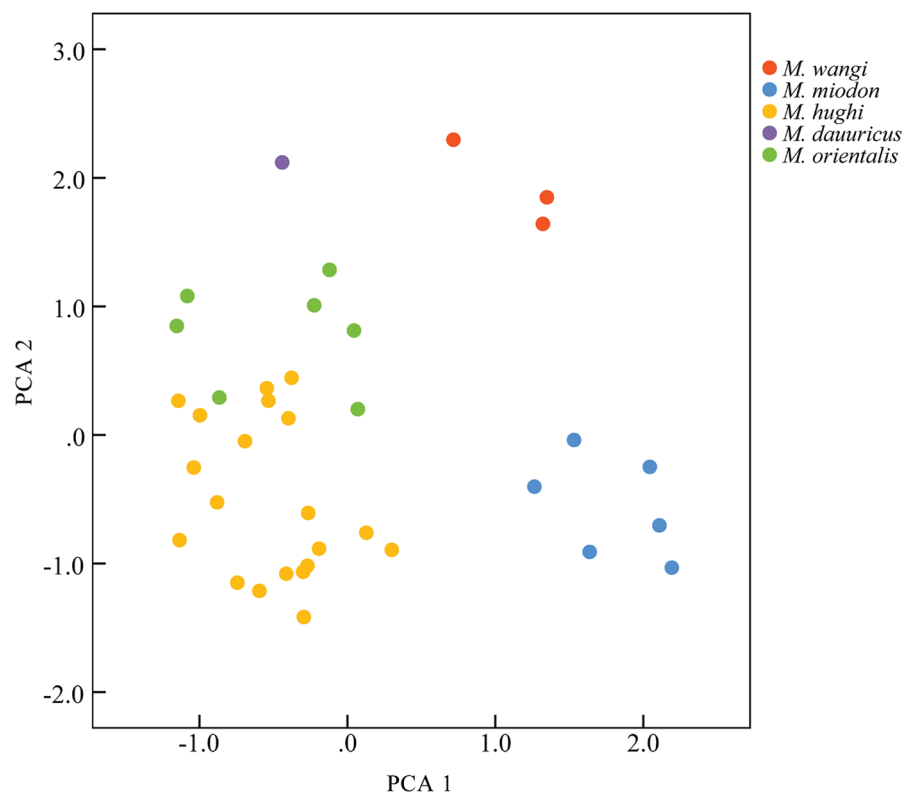


Figure 3. Plot of *Mesechinus orientalis* sp. nov. for PCA 1 and PCA 2.

Table 2. External and cranial measurements (mm) of *Mesechinus* specimens examined; mean \pm S), range for each measurement, and number of specimens measured (*n*) are given.

	<i>M. orientalis</i> sp. nov.	<i>M. hughi</i>	<i>M. dauricus</i>	<i>M. miodon</i>	<i>M. wangi</i>
	<i>n</i> = 7	<i>n</i> = 31	<i>n</i> = 13	<i>n</i> = 18	<i>n</i> = 4
W	339 \pm 52.97	341 \pm 125.75	562 \pm 124.31	505 \pm 154.03	401 \pm 43.27
	299–414; 3	112–750; 31	423–840; 11	230–750; 6	336–449; 4
HB	188.83 \pm 8.13	189.71 \pm 23.80	373.91 \pm 21.35	205 \pm 23.53	208.75 \pm 21.90
	176–198; 6	148–232; 31	175–261; 12	120–220; 17	180–140; 4
TL	23.50 \pm 3.77	19.23 \pm 3.26	24.08 \pm 3.50	33.22 \pm 5.07	17.08 \pm 1.78
	16–27; 6	12–24; 27	17–30; 12	25–43; 17	14–18; 4
HF	36.75 \pm 3.19	37.97 \pm 4.29	34.74 \pm 7.08	58.80 \pm 82.43	47.00 \pm 1.12
	31–40; 6	30–47; 31	18–41; 12	35–38; 16	45–48; 4
EL	26.00 \pm 2.66	22.94 \pm 3.93	31.19 \pm 3.28	28.81 \pm 3.03	30.00 \pm 1.49
	23–30; 6	16–33; 31	22–34; 11	24–35; 17	28–31; 4
GLS	49.95 \pm 1.69	49.39 \pm 1.54	55.18 \pm 3.07	54.10 \pm 2.10	54.75 \pm 0.70
	47.64–51.76; 7	45.10–52.40; 23	50.20–58.40; 12	49.30–57.20; 14	53.70–55.60; 4
CBL	49.49 \pm 1.64	48.46 \pm 1.58	54.72 \pm 2.83	53.18 \pm 2.35	54.55 \pm 0.59
	47.27–51.42; 7	44.40–51.20; 23	49.40–57.40; 13	48.50–56.30; 11	53.60–55.20; 4
CH	15.42 \pm 0.54	16.14 \pm 0.95	17.76 \pm 2.00	18.67 \pm 0.66	17.13 \pm 0.60
	14.46–16.39; 7	14.90–18.20; 21	17.20–19.10; 9	17.80–19.70; 6	16.10–17.60; 4
BL	46.66 \pm 1.45	45.55 \pm 1.29	51.83 \pm 1.94	49.64 \pm 2.04	50.00 \pm 1.37
	44.47–48.28; 7	43.20–48.80; 21	48.10–54.50; 13	44.70–52.30; 14	47.70–51.30; 4
PL	27.46 \pm 0.77	26.58 \pm 0.62	28.60; 1	28.82 \pm 1.41	30.25 \pm 0.50
	26.17–28.52; 7	25.70–28.40; 21		27.00–32.18; 14	29.50–30.80; 4
ZMB	29.62 \pm 1.51	28.90 \pm 1.68	32.62 \pm 2.82	32.77 \pm 2.09	33.97 \pm 0.19
	27.78–31.41; 7	25.70–32.00; 22	28.40–36.40; 13	28.70–37.08; 14	33.70–34.10; 3
IOB	12.29 \pm 0.43	12.51 \pm 0.50	13.86 \pm 0.68	13.87 \pm 0.76	14.68 \pm 0.33
	11.51–12.95; 7	11.70–13.60; 23	13.00–15.10; 9	12.90–15.10; 6	14.20–15.10; 4
MTW	24.68 \pm 1.00	21.67 \pm 1.57	25.58; 1	25.93 \pm 1.18	25.60 \pm 0.64
	23.66–26.38; 7	19.50–24.50; 21		24.30–28.30; 14	24.70–26.20; 4
GWN	3.07 \pm 0.29	2.97 \pm 0.29	2.96; 1	2.70 \pm 0.21	4.30 \pm 0.00
	2.70–3.51; 7	2.60–3.60; 23		2.37–2.94; 6	4.30–4.30; 3
BM1	19.54 \pm 0.64	17.38 \pm 0.75	20.20; 1	21.08 \pm 0.66	21.43 \pm 0.25
	19.20–20.27; 7	16.50–19.50; 21		20.30–22.30; 14	21.10–21.70; 3
LUTR	25.27 \pm 0.51	24.65 \pm 1.12	27.85 \pm 1.25	27.25 \pm 0.99	27.90 \pm 1.02
	24.45–25.89; 7	21.40–26.10; 23	25.00–29; 13	25.70–29.02; 14	26.70–29.10; 4
LBTR	22.32 \pm 1.02	21.19 \pm 0.78	24.30; 1	24.91 \pm 0.70	24.85 \pm 0.44
	21.31–24.16; 7	20.20–23.70; 21		23.40–25.70; 14	24.20–25.30; 4

Morphological characteristic matrix

The morphological characteristics matrix is summarized in Suppl. material 3, and the specific characters represented by each number are interpreted in Suppl. material 4. Based on the matrix, *M. orientalis* sp. nov. differs from the most morphologically similar species, *M. hughi* in several characteristics: (1) the parietal is relatively higher than the frontals (frontals more elevated than parietals in *M. hughi*; character 32 in Suppl. material 3); (2) the posterior palatal spine is

Table 3. Factor loading eigenvalues and percentage of variance explained for PC1 and PC2 from principal component analysis.

Variables	Component	
	1	2
BL	0.964	-0.107
CBL	0.956	-0.143
GLS	0.944	-0.208
LUTR	0.922	-0.090
PL	0.910	0.165
LBTR	0.895	0.100
BM1	0.874	0.251
ZMB	0.832	0.020
IOB	0.791	-0.022
MTW	0.745	0.306
GWN	0.308	0.715
CH	0.591	-0.642
Eigenvalues	8.294	1.210
Variance explained (%)	69.116	10.081

vestigial (vs spine is well developed in *M. hughi*; character 25); (3) suprameatal fossa is moderately developed (vs shallow in *M. hughi*; character 30); (4) P² is two-rooted and not completely fused (Fig. 4) (the single root or two roots of P² are well fused in *M. hughi*; character 73); (5) P³ is small because of a vestigial protocone (vs larger and with protocone well developed in *M. hughi*; character 82).

Phylogenetic relationships

The ML and BI trees showed identical topologies, and only the BI tree is shown (Fig. 5). Relationships among all *Mesechinus* species were strongly supported (PP = 1.00). *Mesechinus orientalis* sp. nov. is strongly supported as embedded within the *Mesechinus* clade (PP = 1.00). Among the *Mesechinus* species, the new species forms a sister relationship (PP = 1.00) to the *M. hughi* + *M. wangi* clade, whose sister relationship was also strongly supported (PP = 1.00).

Divergence times

Divergence time estimates show that the most recent common ancestor of *Mesechinus* occurred in the early Pleistocene, ca 1.71 Ma (95% CI = 1.23–2.24 Ma) (Fig. 6). *Mesechinus orientalis* sp. nov. diverged from the *M. hughi* + *M. wangi* ancestor ca 1.10 Ma (95% CI = 0.78–1.47 Ma), with *M. hughi* and *M. wangi* diverging ca 0.74 Ma (95% CI = 0.50–1.02 Ma).

Karyotypic characteristics of *Mesechinus orientalis* sp. nov.

The comparison of the G-banding chromosomes of *M. orientalis* sp. nov. and *M. wangi* is shown in Fig. 7. Since the specimen was a female individual,

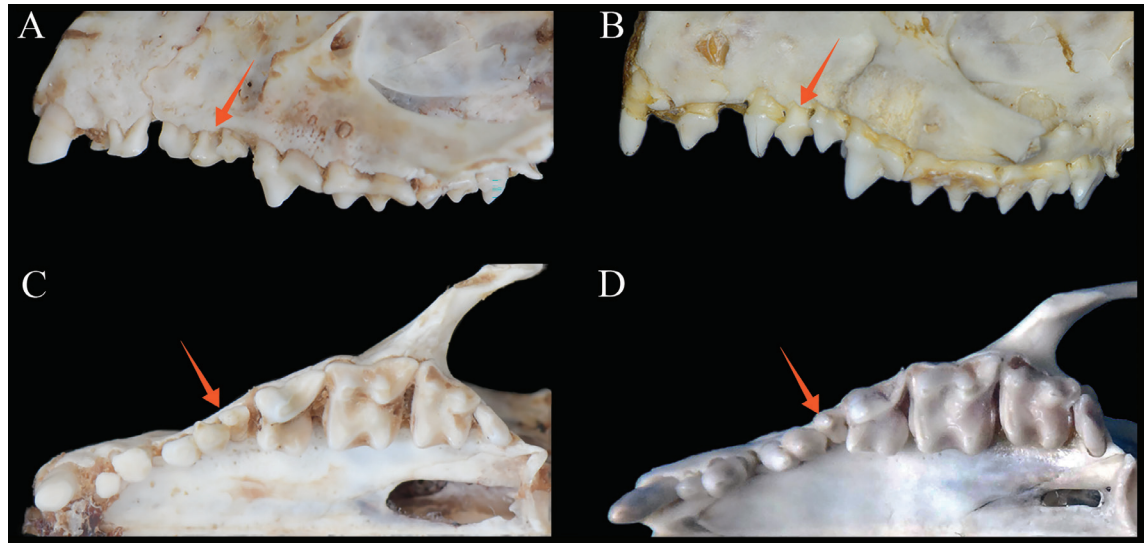


Figure 4. Ventral and lateral views of left upper tooththrow of *M. orientalis* sp. nov. **A, C, B, D** *M. hughi*. The arrows point at the root of P² (**A, B**), and the protocone of P³ (**C, D**).

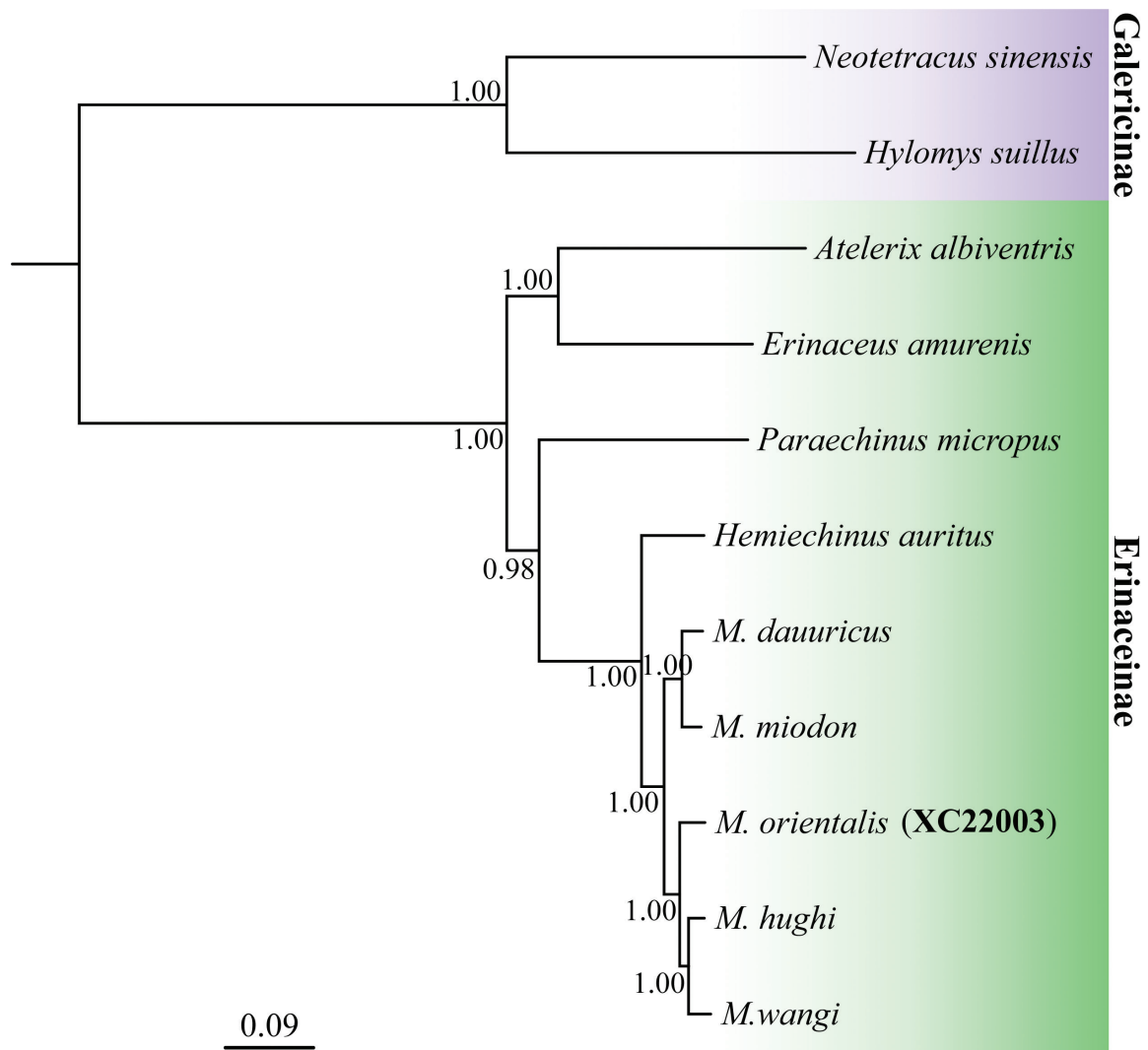


Figure 5. Mitochondrial gene tree of the genus *Mesechinus* and other genera of Erinaceinae and the outgroup. Branch lengths represent substitutions per site. Numbers above branches are posterior probability supporting the relationship.

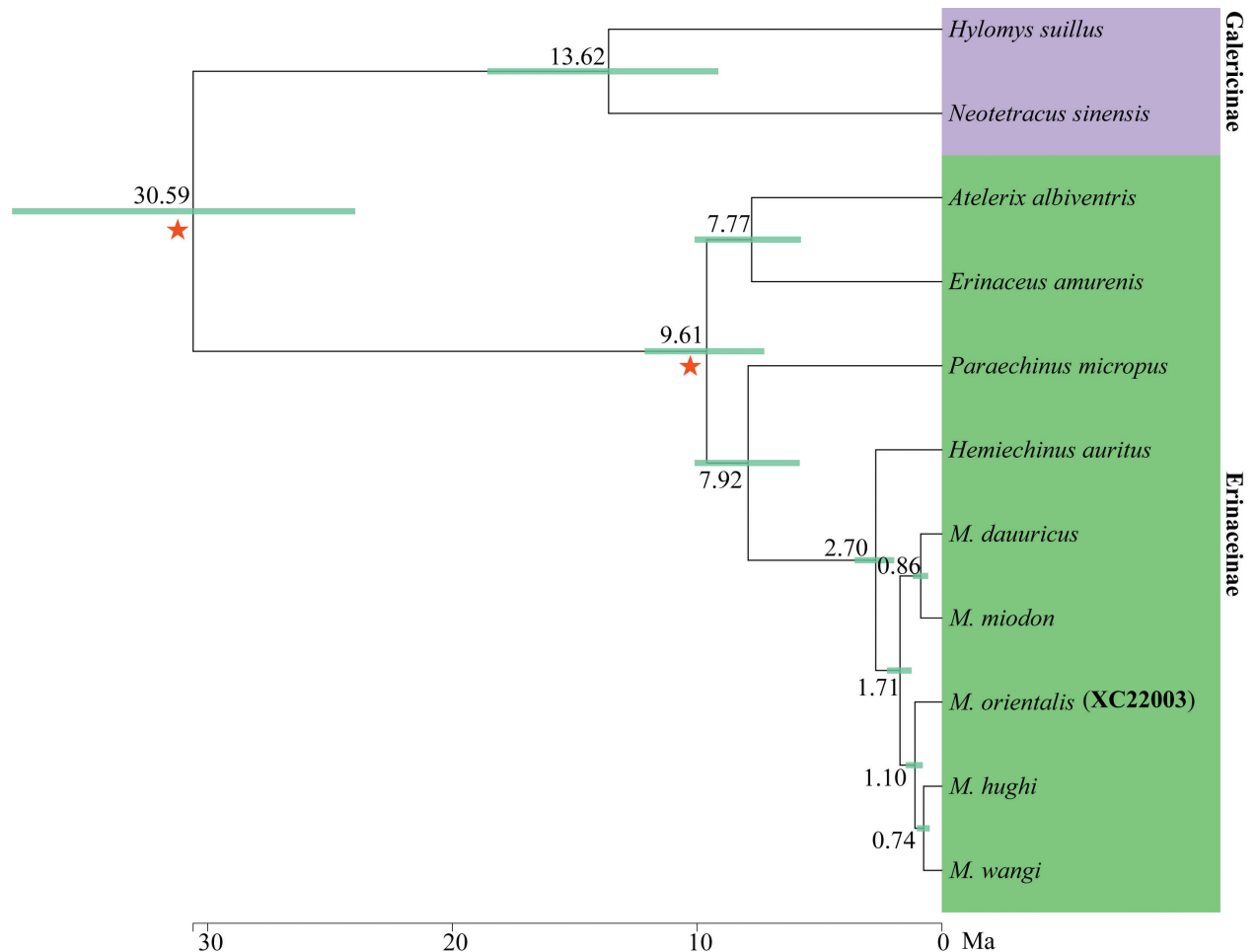


Figure 6. Divergence times estimated using BEAST based on mitogenome data. Branch lengths represent time. Numbers above branches refer to divergence time in millions of years. Asterisks indicate the location of correction points.

its X chromosome was determined by comparing its karyotype with that of *M. wangi*. The two species' autosomes are almost identical; the diploid number (2n) and autosomal fundamental number (FNa) are 48 and 92, respectively. The only difference was the X chromosome, where that of *M. wangi* was meta centric, while that of *M. orientalis* sp. nov. was submetacentric.

Based on the morphological, morphometric, and molecular evidence and the modern phylogenetic species concept (phylogenetic species concept based on both diagnosability and monophyly as operational criteria) (Mayden 1997; Gutiérrez and Garbino 2018), we recognize the *Mesechinus* population from Anhui as a new species and formally describe it below.

Taxonomic account

Mesechinus orientalis sp. nov.

<https://zoobank.org/BB3A29EC-F0A8-4DFD-A954-D5AC8E03B4B2>

Suggested common name. Eastern Forest Hedgehog, 华东林猬 (Huadong Linwei).

Type materials. Holotype: XC 23001, an adult male collected from Xikou Town (30°34'42"N, 118°41'47"E), Xuancheng City, southern Anhui, China, Zifan Shi leg.,

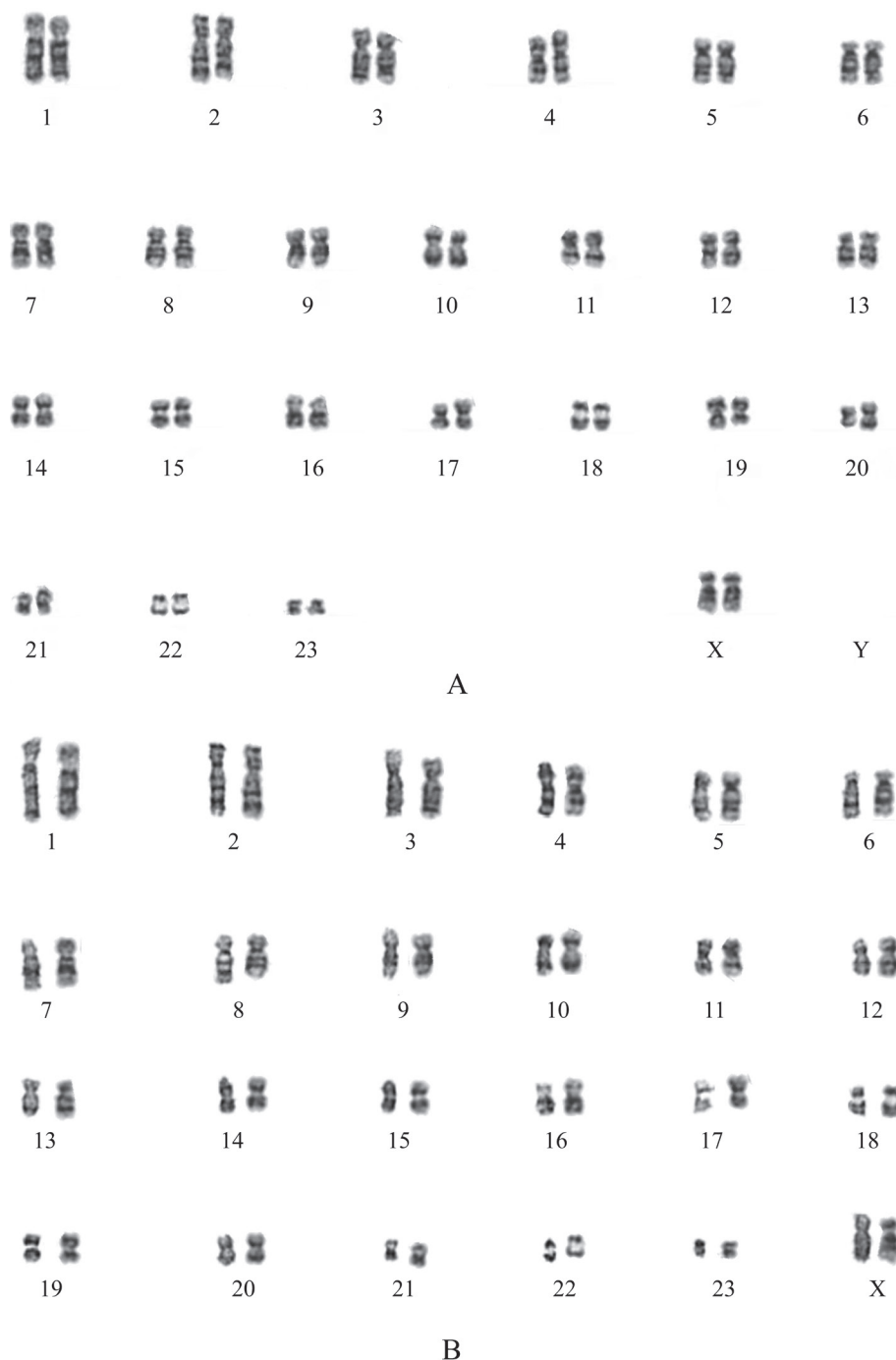


Figure 7. Comparison of karyotypes in two *Mesechinus* species **A** *M. orientalis* sp. nov. (XC 2205003) **B** *M. wangi*.

May 2023. The dried skin, cleaned skull, and tissue samples are deposited in AHNU. **Paratypes:** XC 18001, XC 2205001, XC 2205003, XC 2205005, XC 2205006, HZ 22001, six adult specimens collected from southeast Anhui and northwest Zhejiang, China, between 2018 and 2023. The specimens are deposited in AHNU.

Etymology. The specific name *orientalis* is derived from the Latin *oriens*, “the east”, and suffix *-alis*, “pertaining to”, in reference to the new species’ eastern distribution in Anhui and Zhejiang provinces in eastern China.

Diagnosis. This is a small-bodied hedgehog (GLS = 49.95 ± 1.69 mm), similar to *M. hughi*, but smaller than other *Mesechinus* species. It has the shortest

spines in the genus (18–20 mm); the spines have four-colour rings, similar to the spines of *M. dauuricus* and *M. hughi*, but different from those of *M. miodon* and *M. wangi* (Fig. 8). The parietal is higher than the frontals, which differs from that of *M. hughi* and *M. wangi* (Fig. 9). The P² is two-rooted and not completely fused (Fig. 4). The protocone of P³ is vestigial, which differs from that of *M. hughi*, and smaller than P², which distinguishes it from *M. dauuricus*. The dental formula of *M. orientalis* sp. nov. [I 3/2, C1/1, P 3/2, M 3/3 (×2) = 36], which distinguishes it from *M. wangi*.

Description. This is a small-bodied *Mesechinus* species (HB = 188.83 mm; GLS = 49.95 mm) (Table 2). The ears are small and nearly the same length as the surrounding spines (Fig. 8). The nose is brown, with black whiskers on the snout; these whiskers shorten towards the nose. The spines are the shortest (18–20 mm) among *Mesechinus* species. There are four colour rings on the spine from the base to the tip: two-thirds of the length is white at the base, followed by a 3–4 mm black ring, a narrow light ring, and a black tip (Fig. 8). This species appears to be sexually dimorphic; among the specimens we collected, the pelage of males was generally grey, while that of most of the females (2 of 3 specimens) was reddish brown. However, this is a relatively small sample size, and further investigation is required to establish sexual dimorphism with more certainty.

The skull is heavy and with a shortened rostrum, and the lambdoidal crest is evident. The parietal is relatively higher than the frontal (Fig. 9). On the ventral side of the skull, a posterior palatal shelf and vestigial posterior palatal spine (<1 mm) extend slightly posteriorly. The suprameatal fossa is moderately developed and has the anterior and posterior rim nearly parallel, giving the fossa a more angular or U-shaped appearance. The zygomatic arches are significantly expanded, and the temporal fossa is large and subrounded. The middle palatine foramen is relatively larger than in other *Mesechinus* species. The coronoid process of the mandible is tall, rising upward from the posterior of the toothrow; the tips are slightly curved to the posterior, and the posterior surface is concave (Fig. 9). The mandibular condyle sits posteriorly below the coronoid process at a nearly 45° angle. The angular process is enlarged, thick, long, and triangulate.

As with other *Mesechinus* species, except *M. wangi* which has an additional M⁴, the dental formula of the new species is I 3/2, C1/1, P 3/2, M 3/3 (×2) = 36. The I¹ is enlarged, I² is much smaller than I¹ and I³, and I³ has two roots. P² also has two roots which are not completely fused. P³ is small (smaller than P²) and has a vestigial protocone. M¹ is slightly larger than M², and M³ is reduced.

Comparison. The hedgehogs from China's Anhui and Zhejiang provinces can be easily classified as *Mesechinus* based on the following morphological characteristics: the absence of pure white spines; relatively small ears, almost similar in length to the surrounding spines; no bare part on the forehead nor at the top of the forehead which divides the spines on the head into two halves; and a U-shaped suprameatal fossa.

Among the *Mesechinus* species, *M. orientalis* sp. nov. is morphologically most similar to *M. hughi*. However, the new species can be distinguished by many characters. *Mesechinus orientalis* sp. nov. has the shortest spines in the genus (18–20 mm), shorter than those in *M. hughi* (22–24 mm). The parietal is relatively higher than the frontals in the new species, whereas the frontals are relatively higher than parietals in *M. hughi*. P² has two roots which are not completely fused

in *M. orientalis* sp. nov., while in *M. hughi* P² the two roots are well fused. The P³ protocone is vestigial in the new species but well developed in *M. hughi*. The posterior palatal spine is vestigial, and the suprameatal fossa is moderately developed in the new species, which differs from the well-developed posterior palatal spine and shallow suprameatal fossa in *M. hughi*. In addition, the MTW and BM¹ of the new species are significantly greater than those of *M. hughi* ($P < 0.01$).

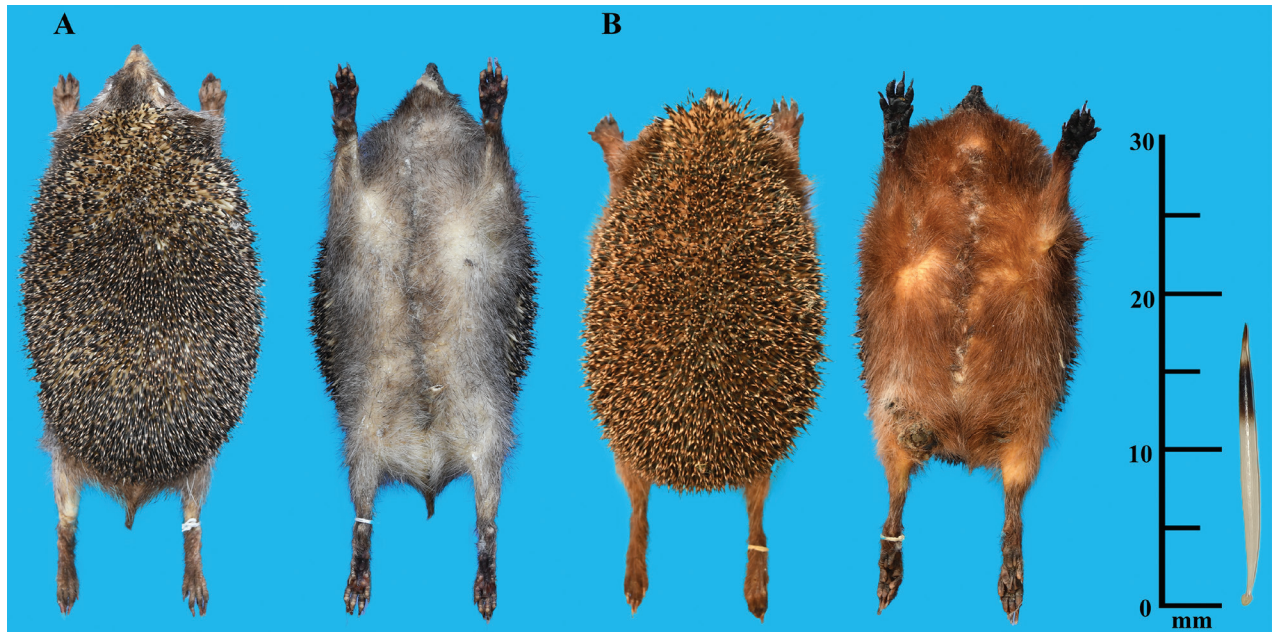


Figure 8. External morphs and spines of *Mesechinus orientalis* sp. nov. **A** male specimen (XC 2205001) **B** female specimen (XC 2205005).

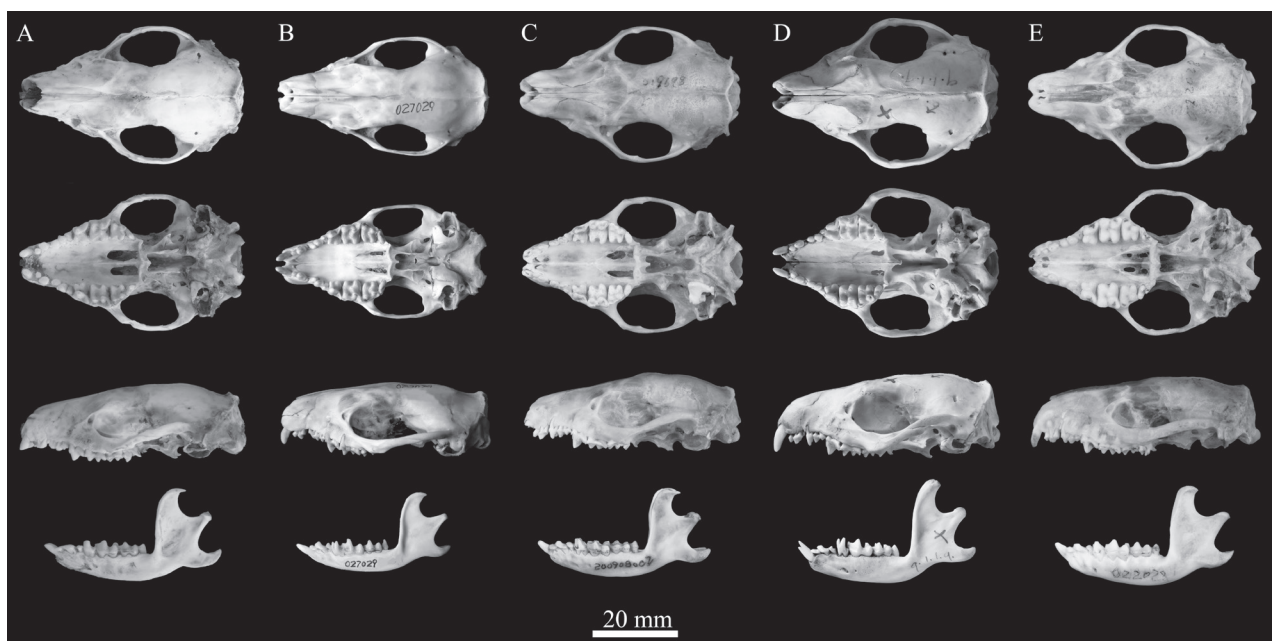


Figure 9. Dorsal ventral and lateral views of skull and mandible of *Mesechinus* species **A** *M. orientalis* sp. nov. (holotype XC 23001) **B** *M. hughi* (KIZ 027029) **C** *M. dauricus* (KIZ 027005) **D** *M. miodon* (holotype BM 9.1.1.9) **E** *M. wangi* (holotype KIZ 022028).

Mesechinus orientalis sp. nov. (HB = 188.83 mm ± 8.13; GLS = 49.95 mm ± 1.69) is distinguishable from *M. dauuricus* (HB = 373.91 mm ± 21.35; GLS = 55.18 mm ± 3.07), *M. miodon* (HB = 205 mm ± 23.53; GLS = 54.10 mm ± 2.10), and *M. wangi* (HB = 208.75 mm ± 21.90; GLS = 54.75 mm ± 0.70) by its smaller size. The spines of the new species are much shorter (18–20 mm) than those of *M. dauuricus* (21–24 mm), *M. miodon* (~26 mm), and *M. wangi* (21–24 mm). The spines of *M. orientalis* sp. nov. have four-colour rings similar to those of *M. dauuricus* and *M. hughi*, but they differ from *M. miodon* and *M. wangi*. P³ of the new species is much smaller than P², which differs from *M. dauuricus*, in which P³ is of equal size to P². The parietal is relatively higher than the frontals in *M. orientalis* sp. nov., which differs from *M. wangi*. Additionally, the presence of M⁴ in *M. wangi* is unique in the genus, which easily distinguishes it from other species.

Distribution and habitat. *Mesechinus orientalis* sp. nov. is currently known from southern Anhui (Xuancheng and Huangshan) and northwestern Zhejiang (Anji, Changxing, Deqing, Yuhang, Linan, Chunan), both in eastern China. Most specimens were collected in scrubland and subtropical broad-leaf evergreen forests at elevations from 30 to 700 m a.s.l.

Discussion

For a long time, the genus *Mesechinus* was thought to be restricted to northern China and adjacent Mongolia and Russia (Wilson and Reeder 2005) until Ai (2007) reported a small population of *Mesechinus* from Mount Gaoligong in Yunnan Province, southwestern China. This Mount Gaoligong population was subsequently described as a new species, *M. wangi* (Ai et al. 2018). In this study, we recognized a population of *Mesechinus* from eastern China as another isolated species, *M. orientalis* sp. nov. Morphologically, the new species is most similar to *M. hughi*, but it is distinguishable from all recognized *Mesechinus* species in having the shortest spines, an incompletely fused two-rooted P², and a smaller, vestigial P³. The new species is geographically isolated from its congeners by at least 1000 km, and it is currently the southeasternmost species of *Mesechinus* (Fig. 1). Except for *M. orientalis* sp. nov., only one species of hedgehog, *Erinaceus amurensis* Schrenk, 1859, occurs in eastern China. While these species are sympatric, at least in Xuancheng, Anhui Province, *M. orientalis* sp. nov. can easily be distinguished from *E. amurensis* by the absence of pure-white spines, and no bare part on the forehead nor at the top of the forehead which divides the spines on the head into two halves (Fig. 8).

The discovery of a new species of *Mesechinus* in eastern China has greatly expanded the known range of the genus and is vital in understanding the macroevolution of the genus. The oldest fossils of *Mesechinus* are from the Early Pleistocene near Taijiaping Village in Nangaoya Township, Tianzhen, Shanxi Province (Bai et al. 2022). Our molecular results reveal that the divergences among *M. orientalis*, *M. wangi*, and *M. hughi* occurred in the Middle Pleistocene 0.74–1.10 Ma (Fig. 6). Increased cooling and aridification during the middle Pleistocene (known as the middle Pleistocene transition at ca 1.2–0.5 Ma) appear to have been critically important in the split of the three species, which may also have facilitated the migration of the ancestors of *M. wangi* and *M. orientalis* sp. nov. to southwestern and southeastern China, respective-

ly. The north–south trending Dabie Mountains, which are located between the Qinling Mountains and southern Anhui, may have provided a migration route for the ancestor of *M. orientalis* sp. nov. to reach southern Anhui. The mountainous area of southern Anhui and northwestern Zhejiang Province also likely acted as glacial refugia in the Pleistocene for the new species.

Acknowledgements

We appreciate the constructive comments and suggestions from the subject editor Alessio Iannucci and the two anonymous reviewers.

Additional information

Conflict of interest

The authors have declared that no competing interests exist.

Ethical statement

Animals were handled complying with the animal care and use guidelines of the American Society of Mammologists, and following the guidelines and regulations approved by the internal review board of Anhui Normal University.

Funding

The study was supported by the National Natural Science Foundation of China (no. 31900318, 32170452), the Science Foundation of Hebei Normal University (No. L2023B54), the Anhui Provincial Natural Science Foundation (2008085QC106), and the University Synergy Innovation Program of Anhui province (GXXT-2020-075).

Author contributions

Conceptualization: ZC, KH. Data curation: ZS, HY, JF. Funding acquisition: ZC, KH, WB. Investigation: ZS, HY, JZ, WN, WS. Project administration: ZC. Resources: ZC, ZS, JZ, SY, XJ. Supervision: ZC, KH, XJ. Visualization: ZS, WS, WN. Writing - original draft: ZS, ZC. Writing - review and editing: ZC, ZS, XJ, KOO, KH, WB.

Author ORCIDs

Zifan Shi  <https://orcid.org/0009-0008-5165-6604>

Kai He  <https://orcid.org/0000-0002-6234-2589>

Jiajun Zhou  <https://orcid.org/0000-0003-1038-1540>

Kenneth O. Onditi  <https://orcid.org/0000-0003-4034-6818>

Xuelong Jiang  <https://orcid.org/0000-0003-2052-2490>

Zhongzheng Chen  <https://orcid.org/0000-0003-3821-0145>

Data availability

All of the data that support the findings of this study are available in the main text or Supplementary Information.

References

Ai HS (2007) A short introduction of the cover photo for the current issue. *Zoological Research* 28(6): 633. <https://www.zoores.ac.cn/en/article/id/39>

- Ai HS, He K, Chen ZZ, Li JQ, Wan T, Li Q, Nie WH, Wang JH, Su WT, Jiang XL (2018) Taxonomic revision of the genus *Mesechinus* (Mammalia: Erinaceidae) with description of a new species. *Zoological Research* 39: 335–347. <https://doi.org/10.24272/j.issn.2095-8137.2018.034>
- Andreychev A, Kuznetsov V (2020) Checklist of rodents and insectivores of the Mordovia, Russia. *ZooKeys* 1004: 129–139. <https://doi.org/10.3897/zookeys.1004.57359>
- Bai W, Dong W, Liu W, Zhang L, Li L, Li Q (2022) Pleistocene Hedgehog *Mesechinus* (Eulipotyphla, Mammalia) in China. *Journal of Mammalian Evolution* 29(4): 797–814. <https://doi.org/10.1007/s10914-022-09612-w>
- Bannikova AA, Matveev VA, Kramerov DA (2002) Using inter-SINE-PCR to study mammalian phylogeny. *Russian Journal of Genetics* 38(6): 714–724. <https://doi.org/10.1023/A:1016056304555>
- Bernt M, Donath A, Jühling F, Externbrink F, Florentz C, Fritzscht G, Pütz J, Middendorf M, Stadler PF (2013) MITOS: Improved de novo metazoan mitochondrial genome annotation. *Molecular Phylogenetics and Evolution* 69(2): 313–319. <https://doi.org/10.1016/j.ympev.2012.08.023>
- Bouckaert R, Heled J, Kühnert D, Vaughan T, Wu CH, Xie D, Suchard MA, Rambaut A, Drummond AJ (2014) BEAST 2: A software platform for Bayesian evolutionary analysis. *PLoS Computational Biology* 10(4): e1003537. <https://doi.org/10.1371/journal.pcbi.1003537>
- Chen ZZ, Tang XF, Tang HY, Zhao HT, Miao QL, Shi ZF, Wu HL (2020) First record of genus *Mesechinus* (Mammalia: Erinaceidae) in Anhui Province, China—*Mesechinus hughi*. *Acta Theriologica Sinica* 40: 96–99. <http://www.mammal.cn/CN/10.16829/j.slxb.150318>
- Corbet GB (1988) The family Erinaceidae: A synthesis of its taxonomy, phylogeny, ecology and zoogeography. *Mammal Review* 18(3): 117–172. <https://doi.org/10.1111/j.1365-2907.1988.tb00082.x>
- de Sena Brandine G, Smith AD (2021) Falco: High-speed FastQC emulation for quality control of sequencing data. *F1000 Research* 8: 1874. <https://doi.org/10.12688/f1000research.21142.2>
- Dierckxsens N, Mardulyn P, Smits G (2017) NOVOPlasty: De novo assembly of organelle genomes from whole genome data. *Nucleic Acids Research* 45: e18. <https://doi.org/10.1093/nar/gkw955>
- Frost DR, Wozencraft WC, Hoffmann RS (1991) Phylogenetic relationships of hedgehogs and gymnures (Mammalia, Insectivora, Erinaceidae). *Smithsonian Contributions to Zoology* 518(518): 1–69. <https://doi.org/10.5479/si.00810282.518>
- Gould GC (1995) Hedgehog phylogeny (Mammalia, Erinaceidae)—The reciprocal illumination of the quick and the dead. *American Museum Novitates* 3131: 1–45. <http://hdl.handle.net/2246/3665>
- Gutiérrez EE, Garbino GS (2018) Species delimitation based on diagnosis and monophyly, and its importance for advancing mammalian taxonomy. *Zoological Research* 39: 301–308. <https://doi.org/10.24272/j.issn.2095-8137.2018.037>
- He K, Eastman TG, Czolacz H, Li S, Shinohara A, Kawada S, Springer MS, Berenbrink M, Campbell KL (2021) Myoglobin primary structure reveals multiple convergent transitions to semi-aquatic life in the world’s smallest mammalian divers. *eLife* 10: e66797. <https://doi.org/10.7554/eLife.66797>
- Kearse M, Moir R, Wilson A, Stones-Havas S, Cheung M, Sturrock S, Buxton S, Cooper A, Markowitz S, Duran C, Thierer T, Ashton B, Meintjes P, Drummond A (2012) Geneious Basic: An integrated and extendable desktop software platform for the organiza-

- tion and analysis of sequence data. *Bioinformatics* 28(12): 1647–1649. <https://doi.org/10.1093/bioinformatics/bts199>
- Korablev VP, Kirilyuk V, Golovushkin MI (1996) Study of the karyotype of daurian hedgehog *Mesechinus dauuricus* (mammalia, erinaceidae) from its terra typica. *Zoologicheskii Zhurnal* [Зоологический журнал] 75: 563–564.
- Kryštufek B, Motokawa M (2018) Talpidae (Moles, desmans, star-nosed moles and shrew moles). In: Wilson D, Mittermeier R (Eds) *Handbook of the Mammals of the World*. Vol. 8: Insectivores, Sloths, Colugos. Lynx Editions, Barcelona, 552–620.
- Lanfear R, Frandsen PB, Wright AM, Senfeld T, Calcott B (2017) PartitionFinder 2: New methods for selecting partitioned models of evolution for molecular and morphological phylogenetic analyses. *Molecular Biology and Evolution* 34: 772–773. <https://doi.org/10.1093/molbev/msw260>
- Mayden R (1997) A hierarchy of species concepts: The denouement in the saga of the species problem. *Systematics Association Special* 54: 381–423.
- Meng G, Li Y, Yang C, Liu S (2019) MitoZ: A toolkit for animal mitochondrial genome assembly, annotation and visualization. *Nucleic Acids Research* 47(11): e63–e63. <https://doi.org/10.1093/nar/gkz173>
- Meredith RW, Janečka JE, Gatesy J, Ryder OA, Fisher CA, Teeling EC, Goodbla A, Eizirik E, Simão TL, Stadler T, Rabosky DL, Honeycutt RL, Flynn JJ, Ingram CM, Steiner C, Williams TL, Robinson TJ, Burk-Herrick A, Westerman M, Ayoub NA, Springer MS, Murphy WJ (2011) Impacts of the Cretaceous Terrestrial Revolution and KPg extinction on mammal diversification. *Science* 334(6055): 521–524. <https://doi.org/10.1126/science.1211028>
- Miller MA, Schwartz T, Pickett BE, He S, Klem EB, Scheuermann RH, Passarotti M, Kaufman S, O’Leary MA (2015) A RESTful API for access to phylogenetic tools via the CIPRES science gateway. *Evolutionary Bioinformatics* 2015: 11. [EBO S21501] <https://doi.org/10.4137/EBO.S21501>
- Müller S (1840) Over de zoogdieren van den Indischen Archipel. In: Temminck CJ (Ed.) *Verhandelingen over de natuurlijke geschiedenis der Nederlandsche overzeesche bezittingen, de Leden der natuurkundige commissie in Indië en andere Schrijvers*. Vol. 3, Zoology. J. Luchtmans en C. C. van der Hoek, Leiden, 9–57.
- Pan QH, Wang YX, Yan K (2007) *A Field Guide to the Mammals of China*. Chinese Forestry Publishing House, Beijing, 420 pp.
- Pavlinov I, Rossolimo OL (1987) Geographic variation and intraspecific taxonomy of sable (*Martes zibellina* L.) in the USSR. *Mammals. Studying the Soviet Union Fauna* 18: 241–256.
- Rambaut A (2017) FigTree-version 1.4. 3, a graphical viewer of phylogenetic trees. <http://tree.bio.ed.ac.uk/software/figtree>
- Rambaut A, Drummond AJ, Xie D, Baele G, Suchard MA (2018) Posterior summarization in Bayesian phylogenetics using Tracer 1.7. *Systematic Biology* 67(5): 901–904. <https://doi.org/10.1093/sysbio/syy032>
- Schrenk LV (1859) *Reisen und Forschungen im Amur-Lande in den Jahren 1854–1856*. Vol. Bd.1, Commissionäre der K. Akademie der Wissenschaften, St. Petersburg, 212 pp. <https://doi.org/10.5962/bhl.title.15761>
- Sikes RS (2016) Guidelines of the American Society of Mammalogists for the use of wild mammals in research and education. *Journal of Mammalogy* 97(3): 663–688. <https://doi.org/10.1093/jmammal/gyw078>
- Sundevall CJ (1842) Ofversigt af slagtet *Erinaceus*. *Kungliga Svenska Vetenskapssakademien. Handlingar* 1841: 215–239.

- Tamura K, Stecher G, Kumar S (2021) MEGA 11: Molecular Evolutionary Genetics Analysis version 11. *Molecular Biology and Evolution* 38(7): 3022–3027. <https://doi.org/10.1093/molbev/msab120>
- Thomas O (1908) The Duke of Bedford's Zoological Exploration in Eastern Asia.—XI. On mammals from the provinces of Shan-si and Shen-si, northern China. *Proceedings of the Zoological Society of London* 78(4): 963–983. <https://doi.org/10.1111/j.1469-7998.1908.00963.x>
- Trouessart EL (1909) *Neotetracus sinensis*, a new insectivore of the family Erinaceidae. *The Annals and Magazine of Natural History (Series 8)* 4: 389–391. <https://doi.org/10.1080/00222930908692683>
- Wilson DE, Mittermeier RA (2018) *Handbook of the Mammals of the World. Vol. 8: Insectivores, Sloths and Colugos*. Lynx Edicions, Barcelona, 326–327.
- Wilson DE, Reeder DM (2005) *Mammal Species of the World: a Taxonomic and Geographic Reference. Vol. 1*. JHU Press, Baltimore, 2, 142 pp.
- Xie J, Chen Y, Cai G, Cai R, Hu Z, Wang H (2023) Tree visualization by one table (tvBOT): A web application for visualizing, modifying and annotating phylogenetic trees. *Nucleic Acids Research* 51(W1): 587–592. <https://doi.org/10.1093/nar/gkad359>
- Zhang D, Gao F, Jakovlić I, Zou H, Zhang J, Li WX, Wang GT (2020) PhyloSuite: An integrated and scalable desktop platform for streamlined molecular sequence data management and evolutionary phylogenetics studies. *Molecular Ecology Resources* 20(1): 348–355. <https://doi.org/10.1111/1755-0998.13096>

Supplementary material 1

Collection information of *Mesechinus orientalis* sp. nov.

Authors: Zifan Shi, Hongfeng Yao, Kai He, Weipeng Bai, Jiajun Zhou, Jingyi Fan, Weiting Su, Wenhui Nie, Shuzhen Yang, Kenneth O. Onditi, Xuelong Jiang, Zhongzheng Chen
Data type: xlsx

Copyright notice: This dataset is made available under the Open Database License (<http://opendatacommons.org/licenses/odbl/1.0/>). The Open Database License (ODbL) is a license agreement intended to allow users to freely share, modify, and use this Dataset while maintaining this same freedom for others, provided that the original source and author(s) are credited.

Link: <https://doi.org/10.3897/zookeys.1185.111615.suppl1>

Supplementary material 2

Partitioning schemes used in mitogenome RAXML analyses

Author: Zifan Shi

Data type: xlsx

Copyright notice: This dataset is made available under the Open Database License (<http://opendatacommons.org/licenses/odbl/1.0/>). The Open Database License (ODbL) is a license agreement intended to allow users to freely share, modify, and use this Dataset while maintaining this same freedom for others, provided that the original source and author(s) are credited.

Link: <https://doi.org/10.3897/zookeys.1185.111615.suppl2>

Supplementary material 3

Morphological characteristic matrix

Authors: Zifan Shi, Hongfeng Yao, Kai He, Weipeng Bai, Jiajun Zhou, Jingyi Fan, Weiting Su, Wenhui Nie, Shuzhen Yang, Kenneth O. Onditi, Xuelong Jiang, Zhongzheng Chen

Data type: xlsx

Explanation note: Matrix of morphological characters of erinaceid species. The specific characters represented by each number are interpreted in Suppl. material 4.

Copyright notice: This dataset is made available under the Open Database License (<http://opendatacommons.org/licenses/odbl/1.0/>). The Open Database License (ODbL) is a license agreement intended to allow users to freely share, modify, and use this Dataset while maintaining this same freedom for others, provided that the original source and author(s) are credited.

Link: <https://doi.org/10.3897/zookeys.1185.111615.suppl3>

Supplementary material 4

Morphological transformation series

Authors: Zifan Shi, Hongfeng Yao, Kai He, Weipeng Bai, Jiajun Zhou, Jingyi Fan, Weiting Su, Wenhui Nie, Shuzhen Yang, Kenneth O. Onditi, Xuelong Jiang, Zhongzheng Chen

Data type: doc

Copyright notice: This dataset is made available under the Open Database License (<http://opendatacommons.org/licenses/odbl/1.0/>). The Open Database License (ODbL) is a license agreement intended to allow users to freely share, modify, and use this Dataset while maintaining this same freedom for others, provided that the original source and author(s) are credited.

Link: <https://doi.org/10.3897/zookeys.1185.111615.suppl4>